

Accepted Manuscript

Title: Transition metal doped TiO₂ mediated Photocatalytic degradation of anti-inflammatory drug under solar irradiations

Author: Vibhu Bhatia Amit Dhir

PII: S2213-3437(16)30032-X

DOI: <http://dx.doi.org/doi:10.1016/j.jece.2016.01.032>

Reference: JECE 955



To appear in:

Received date: 7-11-2015

Revised date: 21-1-2016

Accepted date: 22-1-2016

Please cite this article as: Vibhu Bhatia, Amit Dhir, Transition metal doped TiO₂ mediated Photocatalytic degradation of anti-inflammatory drug under solar irradiations, Journal of Environmental Chemical Engineering <http://dx.doi.org/10.1016/j.jece.2016.01.032>

This is a PDF file of an unedited manuscript that has been accepted for publication. As a service to our customers we are providing this early version of the manuscript. The manuscript will undergo copyediting, typesetting, and review of the resulting proof before it is published in its final form. Please note that during the production process errors may be discovered which could affect the content, and all legal disclaimers that apply to the journal pertain.

Transition metal doped TiO₂ mediated Photocatalytic degradation of anti-inflammatory drug
under solar irradiations

Vibhu Bhatia, Amit Dhir* amit.dhir@thapar.edu

School of Energy and Environment, Thapar University, Patiala, India-147004

*Corresponding author.

Abstract

Bismuth (Bi) and Nickel (Ni) doped Titanium dioxide (TiO₂) nanoparticles were synthesized by sol-gel method and the prepared nanoparticles were characterized by X-Ray Diffraction, Scanning Electron Microscope, UV-Vis reflectance spectroscopy and Brunauer–Emmett–Teller (BET) analysis. The concentration of dopant in synthesized catalysts was varied from 0.25- 1.0 wt%. Maximum BET surface area of 47.8 and 45.7m²/g was observed with 0.25wt% Bi-TiO₂ and 0.5wt % Ni-TiO₂, respectively. EDX analysis has established the presence of 0.21% Bi ions and 0.36% Ni ions in 0.25wt% Bi doped TiO₂ and 0.5wt% Ni doped TiO₂, respectively. Band gap of Bi-TiO₂ (0.25wt %) and Ni-TiO₂ (0.5wt %) was obtained to be 2.99ev, which is found to be minimum among the various synthesized catalysts. The photocatalytic activity of synthesized catalysts were tested and compared with Degussa TiO₂ for degradation of Ibuprofen (IBP) as a model Compound. Bi-TiO₂ nanoparticles revealed higher photocatalytic activity when compared to Ni-TiO₂ or Degussa TiO₂ under solar irradiation, which may be attributed to increase in specific surface area, and decrease in the crystallite size. Maximum of 89% degradation was achieved with 0.25% Bi-TiO₂ photocatalyst under 6 h of illuminations with a solar light, whereas, 78% degradation has been achieved under similar experimental condition with Ni doped TiO₂. The kinetics of the degradation of IBP has been explained in terms of the Langmuir-Hinshelwood model and was found to follow first order kinetics with k value of 0.0064 and 0.0046 min⁻¹ with Bi and Ni doped TiO₂, respectively.

Keywords: Photocatalysis; Doped; Ibuprofen; Bi-TiO₂; Ni-TiO₂; solar irradiation

1. Introduction

The existence of pharmaceuticals compounds and its residues has been reported frequently in literature (Melo et al. 2009; Halling-Sorensen et al. 1998) thus, receiving increasing attention as an emerging environmental issue. Numerous pharmaceutical compounds have been noticed in household wastewater, natural water bodies and groundwater in many countries all over the world. The Presence of pharmaceutical compounds can cause severe environmental issues due to the chemical toxicity of the lively constituents in the formulations and sometimes, of their disintegration products. Ibuprofen [IBP] is one of the most commonly consumed medicines worldwide, mainly due to its use as a pain reliever. Concentration of IBP in the environment has been stated between 10ng/L to 169µg/L (Santos et al. 2007). Sources of these contaminants are primarily the domestic waste water due to excretion of non-metabolized drugs by animal or human urine and feces. Conventional treatment processes functional at sewage treatment plants are not efficient in removing such pharmaceutical substances by various physical or biological treatment steps. Therefore, alternative and effective treatment methods need to be explored for the degradation of such pharmaceutical compounds.

Several research outcomes have shown favorable results in the exclusion of pharmaceutical pollutants using the application of Advanced Oxidation Processes (AOPs). The AOPs are oxidative processes that have been shown to be efficient for the degradation of several organic compounds based on attack by the hydroxyl radicals ($\bullet\text{OH}$), superoxide radical ($\bullet\text{O}_2^-$), and hydrogen peroxide (H_2O_2) generated by UV-irradiated. (Mendez-Arriagad et al. 2009). The derivatives after AOPs have been reported to be degraded by biological oxidation (Torres et al. 2003).

Although, TiO_2 catalysts are capable of degrading a wide range of organic/inorganic pollutants and toxic materials in all phases such as liquid and gas systems, but the rapid recombination rate of electron-hole pairs generated by photons reduces the commercialization of this technology. For this reason, recent research laid prominence on catalyst doping with transition and noble metals (Torres et al. 2003). Achilleos et al. 2010 investigated the degradation of IBP and carbamazepine using Degussa TiO_2 and it was documented that 60% of compound was degraded within 120min of irradiation time. The presence of metals as dopant, such as Pt, Pd, Au and Ag has been reported to boost the photocatalytic activity of catalyst. Various studies have reported that Bismuth Oxide families such as BiVO_4 , Bi_2O_3 , and Bismuth-doped TiO_2 are remarkable visible light lively photocatalysts for

degradation of organic pollutants, hydrogen generation and dye-sensitized solar cell applications (Tang et al. 2004; Lin et al. 2006; Yu et al. 2008a; Wang et al. 2008; Ji et al. 2009).

The literature studies on the photocatalytic degradation of pharmaceuticals in aqueous streams did not address its photocatalytic oxidation using doped photocatalyst under solar irradiations. Moreover, the suitable concentration of dopant in the photocatalyst needs to be explored for the effective degradation of pharmaceutical drug in aqueous stream. Keeping this in view, the present study focused on the degradation efficiency of IBP using lab synthesized Bi and Ni ions doped TiO_2 with different concentrations of dopants under UV/Solar irradiations and the degradation efficiency was compared with commercially available TiO_2 .

2. Experimental Section

2.1 Materials

All the chemicals used in this study were of analytical grade and were used as such without further purification. Titanium dioxide (TiO_2 (D)) was procured from Degussa Corporation, Germany. Ibuprofen (>99% pure) was obtained from Sigma Aldrich. $\text{Bi}(\text{NO}_3)_3 \cdot 5\text{H}_2\text{O}$ and $\text{Ni}(\text{NO}_3)_2 \cdot 6\text{H}_2\text{O}$ were purchased from Loba Chem, India. Titanium isopropoxide, as source of titanium dioxide, was purchased from Sigma Aldrich. Ethanol, used as solvent, was procured from Merck. All the solutions were prepared with deionized water. Fig 1 showing structure of Ibuprofen.

2.2 Preparation of Bi- TiO_2 and Ni- TiO_2

Doped TiO_2 was prepared using solgel method with Titanium isopropoxide (TIP) as precursor. 2.5ml of TIP was added drop by drop to a solution of 10ml ethanol and 2.5ml acetylacetone at room temperature and stirred for 30 min. Then 2ml distilled water was added to above solution. Calculated amount of $\text{Bi}(\text{NO}_3)_3 \cdot 5\text{H}_2\text{O}$ and $\text{Ni}(\text{NO}_3)_2 \cdot 6\text{H}_2\text{O}$ were added respectively into prepared solution so as to prepare appropriate concentration of dopant and a stable sol was finally obtained after stirring for 2h. Afterwards, concentrated solution was placed at 90°C for drying and dried powder was calcined at 400°C for 2h.

2.3 Characterization of Synthesized catalyst

The powder X-ray diffraction (XRD) was done at room temperature using X-Ray diffractometer ($CuK\alpha\lambda = 0.154\text{nm}$) to study the crystal phase of the products. X-ray diffraction (XRD) patterns were collected using a Philips X-ray diffractometer with monochromatic high-intensity in a 2θ range of $20\text{--}70^\circ$. The crystallite size of the particles was calculated using Scherrer's equation (Eq 1).

$$D = K\lambda / \beta \cos\theta \quad (1)$$

Scanning electron microscope (SEM) images were obtained with Philips SEM Analyzer. The Brunauer–Emmett–Teller surface area was measured using N_2 adsorption/desorption (NOVA2000e) USA at liquid-nitrogen temperature (77 K). Band gap has been evaluated using UV-Vis Diffuse reflectance spectrophotometer of Hitachi U3900H at wavelength range of $190\text{--}800\text{nm}$.

2.4 Photocatalytic Reactor and Degradation Methodology

Ibuprofen (IBP) was subjected to photocatalytic treatment in the presence of synthesized photo catalysts and TiO_2 (D). Photocatalytic activity was assessed in a batch glass reactor under slurry mode. Irradiation was provided by seven UV tubes of 36W (Philips) emitting radiation at around 254nm placed at top of the reactor. Initially photodegradation of IBP (25ppm) was assessed using TiO_2 by varying the catalyst dose from $0.5\text{--}2.5\text{g/L}$ and pH from $3\text{--}10$ under UV/solar irradiations. Afterwards IBP was subjected to photodegradation using various lab synthesized catalyst with varying dopant concentration ($0.25\text{wt}\%$ - $1.0\text{wt}\%$) at 2g/L of catalyst dose at pH 6.0 under UV/solar irradiations. Aliquots of the mixture were taken at different time intervals during the reaction and then analyzed for their absorbance in UV-Vis spectrophotometer at 260 nm . Finally kinetics of the IBP degradation was also studied so as to evaluate rate constant using different photocatalysts. For the solar induced photocatalytic reactions, experiments were carried out in the same reactor placed at terrace in the presence of solar irradiations from 10.00 AM to 4.00 PM in the month of May-June. At regular intervals of 1h , samples were injected out and were analyzed using spectrophotometer. The average intensity of sunlight was found to be in the range of $30\text{--}35\text{ W/m}^2$ during the study period.

The surface adsorption of Ibuprofen on catalyst surface was carried out by dispersing the nanoparticles in solution of model compound with both catalysts in the dark. At regular intervals of 15 mins, sample was pipetted out from the broth for centrifugation to separate nanoparticles and subsequently, the drug concentration in the solution was measured through spectrophotometer analysis. During the adsorption process, turbulence was created in the slurry with the help of a magnetic stirrer with an objective to enhance the mass transfer.

3. Results and Discussion

3.1 Characterization

3.1.1 XRD - X-ray diffraction (XRD) patterns were collected monochromatic high-intensity in a 2θ range of $20-70^\circ$ as shown in Fig 2. No noteworthy shift in XRD peaks of Bi-TiO₂ and Ni-TiO₂ compared with Degussa TiO₂ has been observed indicating that Bi³⁺ did not move in the lattice to substitute Ti⁴⁺ particles. It may be due to higher radius of Bi³⁺ (1.03Å) than that of Ti⁴⁺ (0.68Å). The bismuth in the TiO₂ surface may increase the charge separation. Similar observation has been reported by (Rengraj et al. 2006; Xu et al. 2002) where doping of TiO₂ with Bi did not show any substantial variation in peaks of XRD. The reason for stabilizing Ni doped TiO₂ at lower levels has been credited to the almost similar ionic radius of Ni²⁺ (0.72 Å) to that of Ti⁴⁺ (0.68 Å), which was found to replace some portion of Ti⁴⁺ ions in TiO₂ lattice (Braz et al. 2014; Wang et al. 2012; Wang et al. 1999; Chuang et al. 2011; Lopes et al. 2009).

The morphology of doped photocatalysts was analyzed by SEM. Fig 3 depicted that particles have spherical shape and agglomeration had taken place. The EDS analysis of doped TiO₂ showed significant presence of Ni and Bi in synthesized samples. The analytical results from EDS are in realistic arrangement with 0.25-1.0wt% of Bi³⁺ and Ni ions doped into TiO₂. The elemental records of samples for Ti, O and Bi showed homogeneous distribution of elements and no gathering of Bi ions was detected in the 0.25-1.0wt% range of doped Bi-TiO₂ and Ni-TiO₂. From EDS analysis (Table 1), it has been observed that in 0.25wt% of Bi-TiO₂ and Ni-TiO₂, 0.21 and 0.19% of Bi and Ni ions were present, respectively. Subsequently variations have been found in 0.25-1.0wt% of Bi-TiO₂ and Ni-TiO₂.

3.1.2 BET Surface area

The increase in surface area increases the number of active sites, which further promotes the separation efficiency of the electron–hole pair and subsequently, results in enhanced photocatalytic activity. Upon doping with 0.25wt% Ni, the crystallite size was observed to be 13.84 nm and the surface area value was 41.71 m²/g as shown in Table 2. As the dopant concentration was increased to 0.5wt%, the crystallite size value decreased to 10.3 nm and the surface area value increased to 45.70 m²/g. These results suggest that TiO₂ doped with Ni (<0.5wt%) dopant concentration effectively inhibits TiO₂ grain growth possibly by remaining at boundaries of the grain thereby, increasing the crystallite size and decreasing the surface area (Lin et al. 2006; Begum et al. 2008; Wang et al. 1999; Lopes et al. 2009). The decrease in growth of grain can also be due to the formation of Ni–O–Ti bonds in the doped powders, which inhibits the growth of the crystals. However, decrease in the dopant concentration to 0.25wt%, leads to increase in crystalline size and decrease in surface area of synthesized catalyst.

However In case of Bi-TiO₂ it was observed that the surface area and crystal size was found to be as 47.8m²/g and 12.4nm, respectively for dopant concentration of 0.25wt%. Further, by increasing the dopant concentration from 0.25wt% to 1.0wt%, the decrease in surface area and increase in crystalline size was observed which may likely decrease the photocatalytic activity as shown in Table 3.

3.1.3 Band Gap Energy

The UV-vis diffuse reflectance spectrum of all the compositions are shown in Figure 4. It is evident from the results that the UV-vis diffuse reflectance spectrum of Bi doped TiO₂ and Ni doped TiO₂, gave distinct band gap absorption edges at 422 nm, 415 nm, 405 nm for doped Bi(0.25wt%), Bi(0.50wt%), Bi(1.0wt%), and 413 nm, 418 nm, 412 nm for doped Ni(0.25wt%), Ni(0.50wt%), Ni(1.0wt%), respectively. The corresponding band gap energies were found to be 2.99, 3.05 and 3.08eV for 0.25wt%, 0.50wt%, and 1.0wt% Bi- TiO₂, respectively and 3.02, 2.99 and 3.03 eV for 0.25wt%, 0.50wt% and 1.0wt% Ni doped TiO₂, respectively. At lowest concentration of Bi dopant, the absorption edge shift is maximum and hence, the corresponding calculated band gap energy is minimum. This may be attributed to the fact that when the amount of dopants is small, the metals ions are well incorporated into the

lattice withstanding the evolvement of local strains. On the other hand, when the dopants are in excess, Bi ions cannot enter the TiO₂ lattice but cover on the surface of TiO₂ and leads to the formation of heterogeneity junction. So, Bi (0.25wt %) photocatalysts has lower band gap energy (2.9 eV) within the temperature range in which the photocatalytic experiments were carried out when compared to other dopant concentrations. For Ni-TiO₂ the minimum band gap energy of 2.9eV was obtained with dopant concentration of 0.5wt%. As the concentration of dopant is either increased or decreased from 0.5wt%, increase in the value of band gap energy was noticed, which may be due to formation of layer of dopant over TiO₂, hence, ions might not get inserted into lattice of TiO₂.

3.2 TiO₂ mediated Photocatalytic degradation

In order to obtain baseline data with standard TiO₂ (Degussa), photocatalytic degradation of IBP was carried out in slurry mode under UV irradiation. pH of the initial IBP aqueous solution (25 ppm) was varied from 3-10 and TiO₂ (Degussa) was used as photocatalyst. It was observed (Fig.5 (a)) that the degradation efficiency increased with increase in value of pH up to 6.0 and thereafter, decrease in the degradation was observed. The maximum degradation of IBP was found to be 76% using 2g/L TiO₂ (D) at pH 6.0. This behaviour is attributed to the fact that the pKa value of IBP is 4.4 and it is reported as weak acid. The point of zero charge (pzc) of the TiO₂ (Degussa P25) is at pH 6.8 and TiO₂ surface is positively charged in acidic media (pH < 6.8), whereas it is negatively charged under alkaline conditions (pH > 6.8). Therefore, at acidic pH range, the surface of TiO₂ will be positively charged as well as the carboxyl group of IBP, hence, charge repulsion exists. Moreover, at acidic pH, the higher •OH radicals generated are considered to be in equilibrium with the holes trapped at the TiO₂ surface. At alkaline pH range, IBP and TiO₂ both are negatively charged. Moreover, hydroxyl radicals are rapidly scavenged and they do not have the opportunity to react with model compound so enhanced activity is expected at pH 6-7 (Choina et al. 2013; Zhang et al. 2013).

Catalyst dose of TiO₂ was varied from 0.5-2.5g/L as shown in Fig 5(b). It was observed that increasing the concentration of catalyst from 0.5g/L to 2.5g/L, the degradation efficiency kept on increasing upto 2 g/L indicating the significance of available catalyst surface for degradation on its surface under UV illumination and maximum degradation of 76% was achieved with 2g/L of TiO₂ (D) catalyst. Further, increasing the catalyst concentration beyond 2g/L, the photocatalytic efficiency decreased directing that the optimal photons have been adsorbed. The

amount of catalyst more than the certain limit may not be useful because of chances of aggregation, as well as reduction in irradiation field onto the surface due to increase in the turbidity of the solution. Moreover, at high concentration, there is a decrease in surface area availability for light-harvesting for the generation of h^+ / e^- pairs, induced by accumulation as also explained in previous findings (Neppolian et al. 2002; Martínez et al. 2011).

3.3 Variation in dopant concentration

Insertion of transition metal can serve as electron/hole separator and can eradicate the hasty recombination of excited e^- /hole pair all through photoreaction, resulting in enhancing the efficiency of the TiO_2 photocatalyst. But, this effect is subtle to dopant concentration also. The photocatalytic degradation of IBP (25ppm) was assessed using lab synthesized Bi and Ni doped TiO_2 (2g/L) at pH 6.0 under solar irradiations with varying concentrations of dopant. Dopant concentration was varied from 0.25 to 1.0wt% for both Bi- TiO_2 and Ni- TiO_2 . With (0.25wt %) Bi- TiO_2 concentration, 89% of IBP degradation was observed in 6 h of solar irradiation as shown in Fig 6(a) and as concentration of dopant was raised from 0.25 to 1.0wt%, there was decrease in the degradation efficiency. The deferral effect of increase in Bi content on degradation rate may be credited to destruction of hydroxyl radicals due to entrapment of conduction band e^- by the adsorbed metal ions. However, with Ni- TiO_2 , the maximum degradation of 78% was observed with 0.50wt% dopant concentration and it was observed that on either increasing or decreasing the concentration of dopant from 0.50wt%, there was decrease in degradation efficiency of IBP, which may be because of the increased impact of ions with increased dopant concentration up to certain limit (up to 0.50wt%) and thereafter, the photocatalytic activity reduced due to surface charge separation.

3.4 Variation of type of catalyst

The effect of dopants might not be similar on trapping e^- /holes on the surface or during interface charge transfer because of the different locations of the dopant in the lattice. So, the photocatalytic competence would be different for various types of dopants (Barakat et al. 2004; Pouretedal et al. 2009). In order to compare the efficiency of TiO_2 (D) with lab synthesized Bi and Ni doped TiO_2 , IBP was subjected to photocatalytic degradation at pH 6 with photocatalyst dose of 2g/L under solar irradiations. Degradation of 89% was achieved with Bi- TiO_2 , whereas, only 50 and 74% degradation was achieved with Ni- TiO_2 and TiO_2 (D), respectively, under similar experimental

conditions as shown in Fig 7. The Bismuth in the TiO_2 surface may enhance the charge separation and improves its photocatalytic activity. In order to adjudge the extent of adsorption, experiments were conducted in the dark with Bi and Ni doped catalyst which showed negligible degradation efficiency ($< 5\%$). Thus, the orders of photocatalytic degradation of IBP followed by different catalyst has been observed as $\text{Bi-TiO}_2 > \text{TiO}_2 > \text{Ni-TiO}_2$. The cause for this enhancement has been timidly credited to the overpowering of recombination of electron-hole pairs on the surface of the TiO_2 catalyst by low valence Bi ions. Literature also revealed that among numerous transition metal ion dopants, Bi appears to be efficient dopant as the radius of Bi ions is almost similar to that of Titanium ions, so this metal ion gets fused into Titanium crystal lattice structure, which helps to shift absorbance in visible spectra, and hence, results in increasing the photocatalytic activity (Begum et al. 2008; Sreethawong et al. 2005).

Kinetic studies of degradation of IBP (25ppm) with catalyst dose of 2 g/L at pH 6 were carried out to find the reaction rate constant and order of reaction with Bi- TiO_2 , Ni- TiO_2 and TiO_2 (D) as photocatalyst under solar irradiations. The rates constant were found to be 0.0064, 0.0046 and 0.0043 min^{-1} for Bi- TiO_2 , Ni- TiO_2 and TiO_2 (D), respectively with first order kinetics.

3.5 Comparison of Solar/UV as Light source

Fig 8 shows the comparison of degradation studies of IBP in aqueous solution under two different types of irradiation viz UV/Solar irradiations. It was observed that under UV light the degradation was found to be 76% using TiO_2 (D) (2g/L) at pH 6 after 6 h of luminescence. The maximum degradation of 89% was achieved with Bi- TiO_2 as photocatalyst in 6h with dose of 2g/L at pH 6. With the same catalyst under UV light, only 48% degradation was observed. Therefore, the photogenerated electrons in the excited IBP molecules have sufficient energy to produce the superoxide ion and hydroxyl radicals under solar irradiation. Hence it can be said that doping of catalyst with metal ions can reduce the power consumption as the absorbance spectra get shifted in visible region, therefore sunlight can be used as a cost effective source of irradiation.

4. Conclusion

The photocatalytic degradation of IBP has been studied in presence of doped catalyst under solar irradiations. Bi- TiO_2 nanoparticles exhibited higher photocatalytic activity when compared to Ni- TiO_2 and Degussa TiO_2 during the

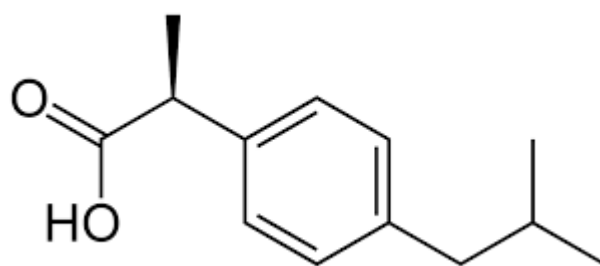
degradation of IBP. The highest BET surface area of Bi-TiO₂ (0.25wt %) was found to be 47.8 m²/g with crystalline size of 12.4 nm. A maximum of 89% IBP degradation was achieved with 0.25 wt% Bi-TiO₂ photocatalyst under 6 h illuminations with a solar light when compared to Ni-TiO₂ wherein, only 78% degradation was achieved under same experimental condition. Among various Ni-doped TiO₂ materials, the one doped with 0.5wt% Ni showed the highest photocatalytic activity for Ibuprofen (IBP) degradation under solar light. The orders of photocatalytic degradation of IBP with different catalyst was observed to be in the order as Bi-TiO₂>TiO₂>Ni-TiO₂ with rate constants as 0.0064 min⁻¹, 0.0046 min⁻¹, 0.0043min⁻¹, respectively.

5. References

1. A. Achilleos, E. Hapeshi, N.P. Xekoukoulotakis, D. Mantzavinos, D. Fatta-Kassinos, UV-A and Solar Photodegradation of Ibuprofen and Carbamazepine Catalyzed by TiO₂, *Separation Sci. & Technol.*, 45 (2010) 1564–1570.
2. N.S. Begum, H.M.F. Ahmed, K.R. Gunashekar, Effects of Ni doping on photocatalytic activity of TiO₂ thin films prepared by liquid phase deposition technique, *Bulletin Mater. Sci.*, 31 (2008) 747-751.
3. M.A. Barakat, H. Schaeffer, G. Hayes, S. Ismat-Shah, Photocatalytic ... Metal ions in photocatalytic systems, *Appl. Catal. B Environ.*, 57 (2004) 23-30.
4. S.H. Chuang, M.L. Hsieh, S.C. Wu, H.C. Lin, T.S. Chao, T.H. Hou, Fabrication and characterization of high-k dielectric nickel titanate thin films using a modified sol-gel method, *J. American Ceramic Society*, 94 (2011) 250–254.
5. J. Choina, H. Kosslick, C. Fischer, G.U. Flechsig, L. Frunza, A. Schulz, Photocatalytic Decomposition of Pharmaceutical Ibuprofen Pollutions in Water over Titaniacatalyst, *Appl. Catal. B: Environmen*, 129 (2013) 589- 598.
6. J.B. Halling-Sorensen, S. Nors Nielsen, P.F. Lanzky, F. Ingerslev, H.C. HoltenLiitzhofl, S.E. Jorgensen, Occurrence, Fate and Effects of Pharmaceutical Substances in the Environment—A Review, *Chemosphere*, 36 (1998) 357- 393.
7. T. Ji, F. Yang, Y. Lv, J. Zhou, J. Sun, Synthesis and visible light photocatalytic activity of Bi-doped TiO₂ nanobelts, *Mater Lett*, 63 (2009) 2044–2046.
8. Y.J. Lin, Y.H. Chang, W.D. Yang, B.S. Tsai, Synthesis and characterization of ilmenite NiTiO₃ and CoTiO₃ prepared by a modified Pechini method, *J. Non-Crystalline Solids*, 352 (2006) 789–794.

9. K.P. Lopes, L.S. Cavalcante, A.Z. Simoes, J.A. Varela, E. Longo, E.T. Leite, NiTiO₃ powders obtained by polymeric precursor method: synthesis and characterization, *J. Alloys and Compounds*, 468 (2009) 327–332.
10. C. Martínez, L.M. Canle, M.I. Fernández, J.A. Santaballa, J. Faria, Kinetics and Mechanism of Aqueous Degradation of Carbamazepine by Heterogeneous Photocatalysis Using Nanocrystalline TiO₂, ZnO and Multi-Walled Carbon Nanotubes—Anatase Composites, *Appl. Catal. B: Environmen*, 102 (2011)563-571.
11. S.A.S Melo, A.G. Trovo, I.R. Bautitz, R.F.P. Nogueira, Degradation of Residual Pharmaceuticals by Advanced Oxidation Processes, *Química Nova* 32 (2009) 188-197.
12. F. Mendez-Arriagad, R.A. Torres-Palma, C. Petriera, S. Esplugasd, J. Gimenezd, C. Pulgarin, Mineralization enhancement of a recalcitrant pharmaceutical pollutant in water by advanced oxidation hybrid processes, *Water Res* 43 (2009) 3984–3991.
13. B. Neppolian, H.C. Choi, S. Sakthivel, B. Arabindoo, V. Murugesan, Solar/UV-Induced Photocatalytic Degradation of Three Commercial Textile Dyes, *J. Hazard. Mater* 89 (2002) 303-317.
14. H. Pouretedal, A. Norozi, M.H. Keshavarz, A. Semnani, Nanoparticles of zinc sulfide doped with manganese, nickel and copper as nanophotocatalyst in the degradation of organic dyes, *J Hazard Mater* 162 (2009) 674-681.
15. S. Rengraj, X.Z. Li, P.A. Tanner, Z.F. Pan, G.K.H. Pang, Photocatalytic degradation of methylparathion – An endocrine disruptor by Bi³⁺ doped TiO₂, *J. mol. Chem. A: Chem* 247 (2006) 36-43
16. J.L. Santos, L. Aparicio, E. Alonoso, Occurrence and risk assessment of pharmaceutically active compounds in waste water treatment plants A case study: seville city(spain), *Environ. Int* 33 (2007) 596-601.

17. T. Sreethawong, Y. Suzuki, S. Yoshikawa, Photocatalytic evolution of hydrogen over mesoporous TiO₂ supported NiO₂ photocatalyst prepared by single-step sol-gel process with surfactant template, *Intern. J. Hydrogen Ener* 30 (2005) 1053–1062.
18. J.W. Tang, Z.G. Zou, J.H. Ye, Efficient photocatalytic decomposition of organic contaminants over CaBi₂O₄ under visible-light irradiation, *Angew Chem Int* 43 (2004) 4463–4466.
19. R. Torres, V. Sarria, W. Torres, P. Peringer, C. Pulgarin, Electrochemical treatment of industrial wastewater containing 5-amino-6-methyl-2-benzimidazolone: toward and electrochemical–biological coupling, *Water Res* 37 (2003) 7–13.
20. Y. Wang, Y. Hao, H. Cheng, Photoelectrochemistry of transition metal-ion-doped TiO₂ nanocrystalline electrodes and higher solar cell conversion efficiency based on Zn²⁺-doped TiO₂ electrode, *J. Mater. Sci.* 34 (1999) 2773–2779.
21. J. Wang, L. Jing, L. Xue, Y. Qu, H. Fu, Enhanced activity of bismuth-compounded TiO₂ nanoparticles for photocatalytically degrading rhodamine B solution, *J Hazard Mater* 160 (2008) 208–212
22. X.H. Xu, M. Wang, Y. Hou, W.F. Yao, D. Wang, H. Wang, Preparation and characterization of Bi-doped TiO₂ photocatalyst, *J Mater Sci Lett* 21 (2002) 1655–1656.
23. J. Yu, S. Liu, Z. Xiu, W. Yu, G. Feng, Combustion synthesis and photocatalytic activities of Bi³⁺-doped TiO₂ nanocrystals, *J Alloys Compd* 461 (2008a) 17–19.

Figure Captions**Fig. 1: Structure of Ibuprofen**

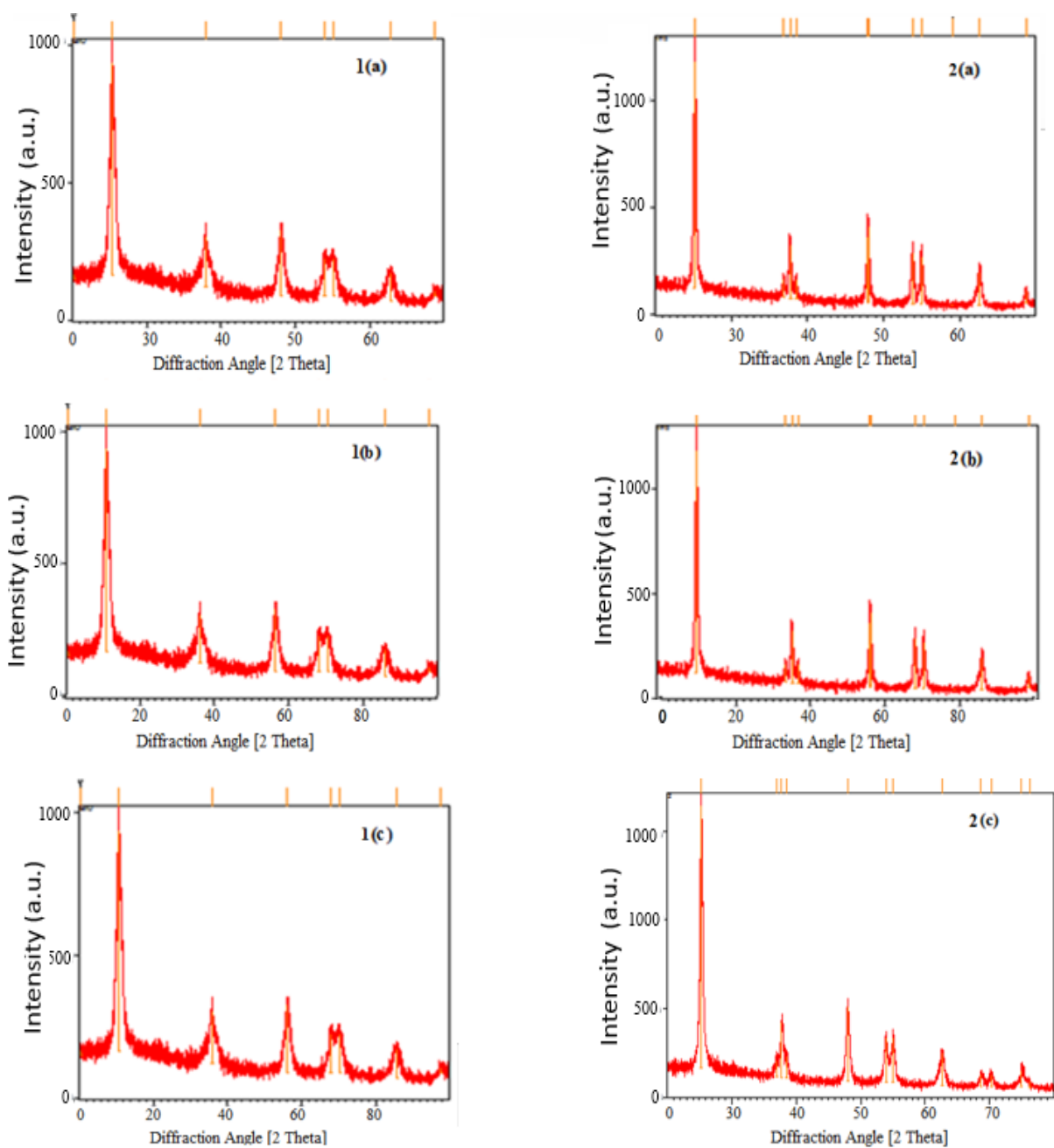


Fig. 2: XRD Pattern of synthesized (1a) 0.25wt% Ni-TiO₂ (1b) 0.5wt% Ni-TiO₂ (1c) 1.0wt% Ni-TiO₂, (2a) 0.25wt% Bi-TiO₂ (2b) 0.5wt% Bi-TiO₂ (2c) 1.0wt% Bi-TiO₂

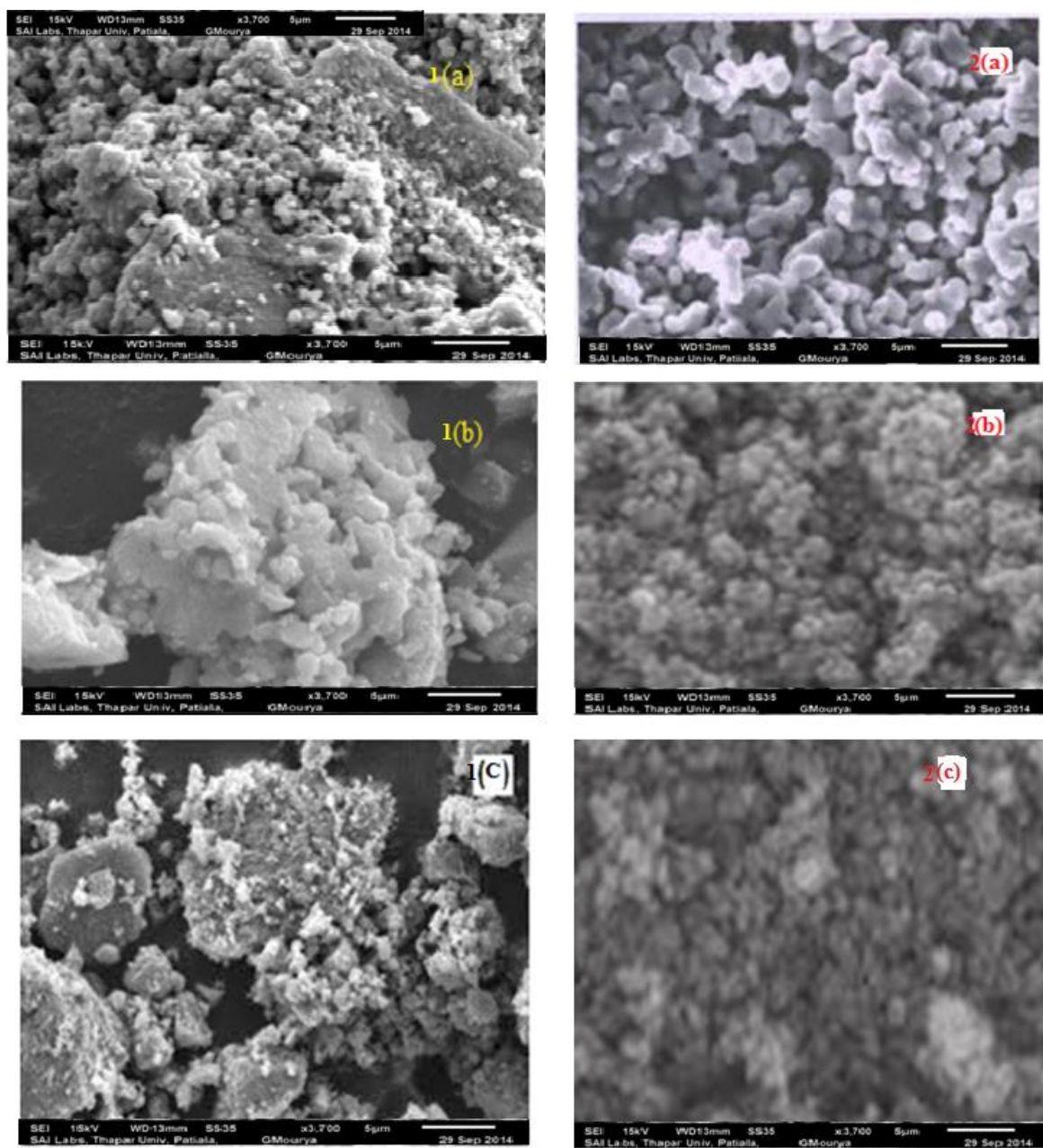


Fig. 3: SEM images of synthesized (1a) 0.25wt% Ni-TiO₂ (1b) 0.5wt% Ni-TiO₂ (1c) 1.0wt% Ni-TiO₂, (2a) 0.25wt% Bi-TiO₂ (2b) 0.5wt% Bi-TiO₂ (2c) 1.0wt% Bi-TiO₂

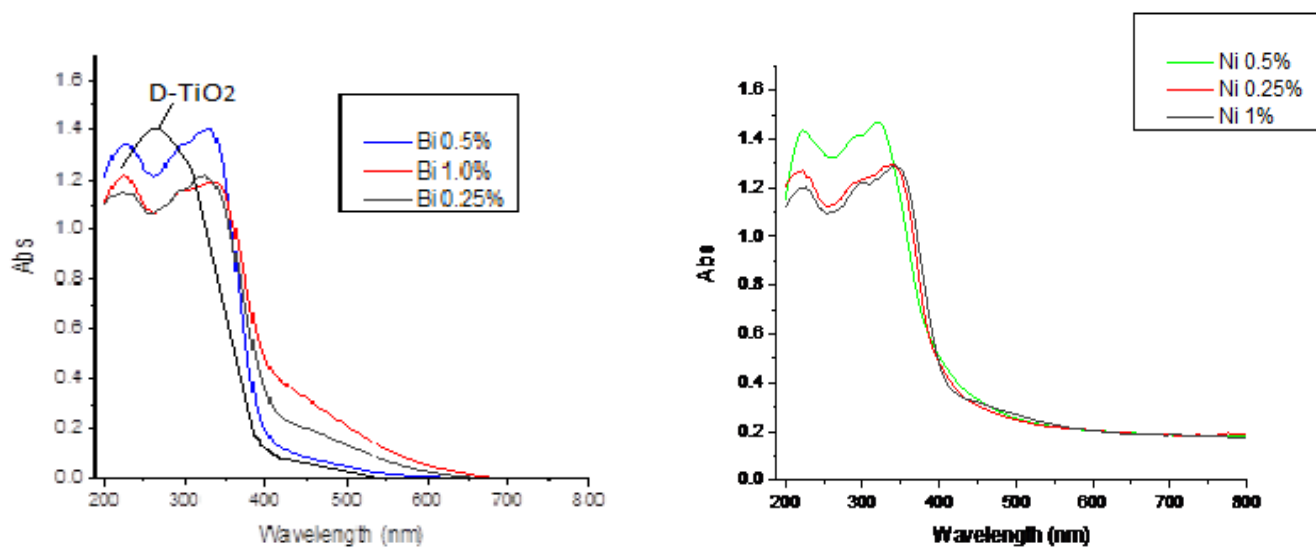


Fig. 4: UV-vis diffuse reflectance spectrum of (a) Bi-TiO₂ (b) Ni-TiO₂

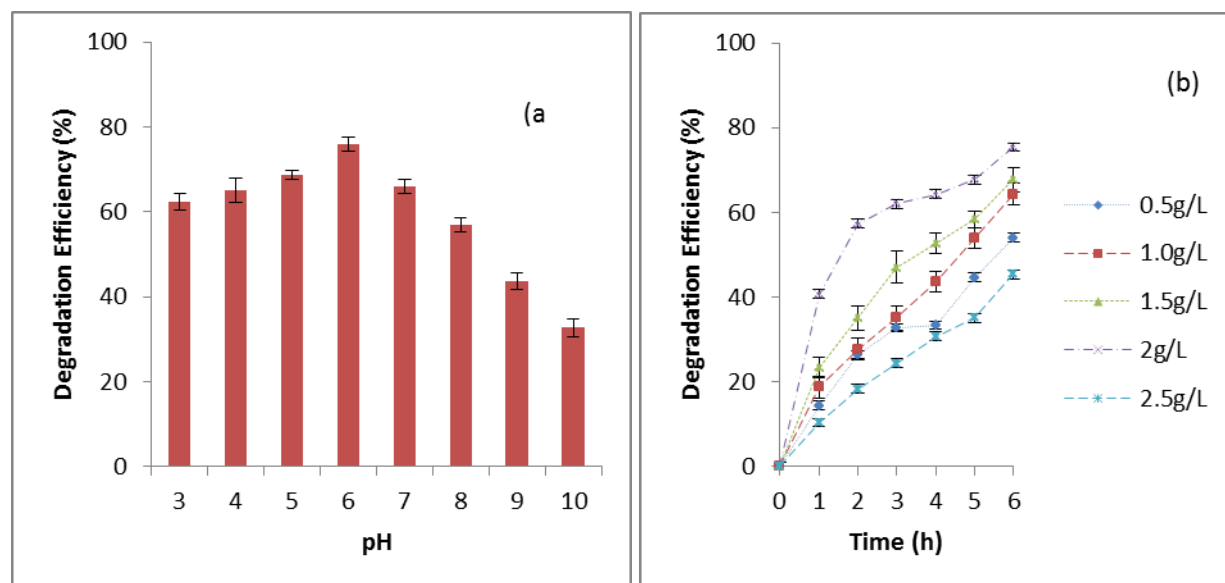


Fig. 5: Effect of photocatalytic parameters (a) Variation of pH (b) Variation of catalyst Dose

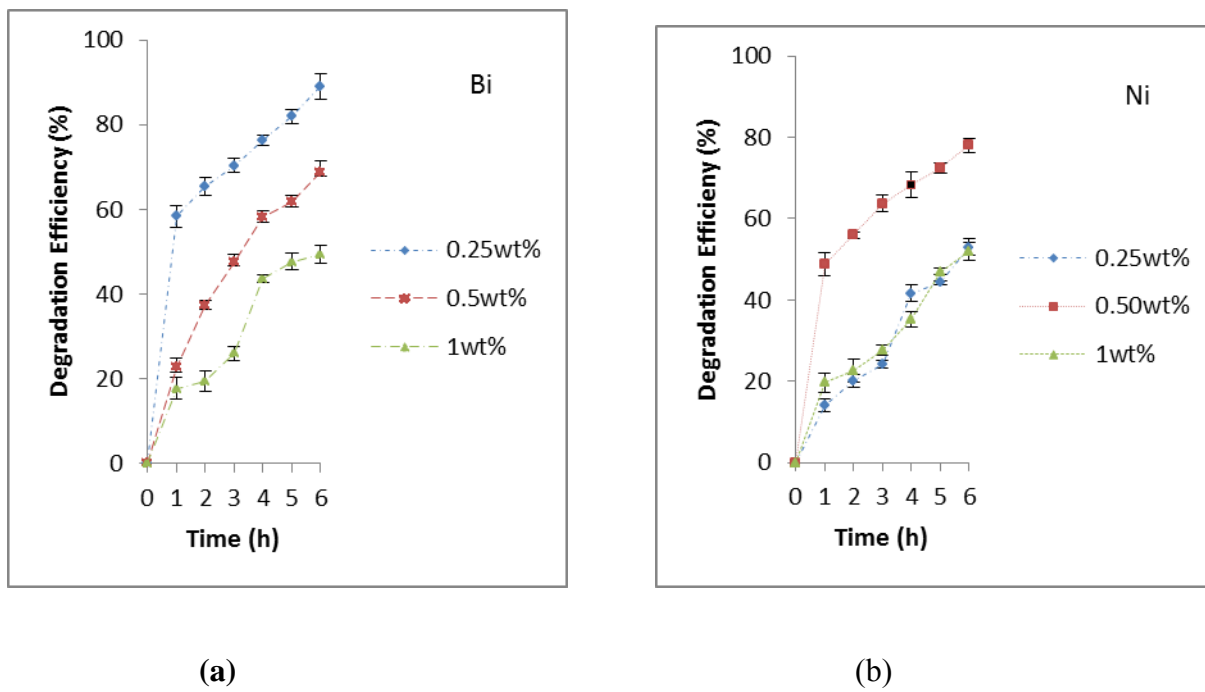


Fig. 6: Variation of dopant concentration (a) Bi (TiO₂) (b) Ni (TiO₂)

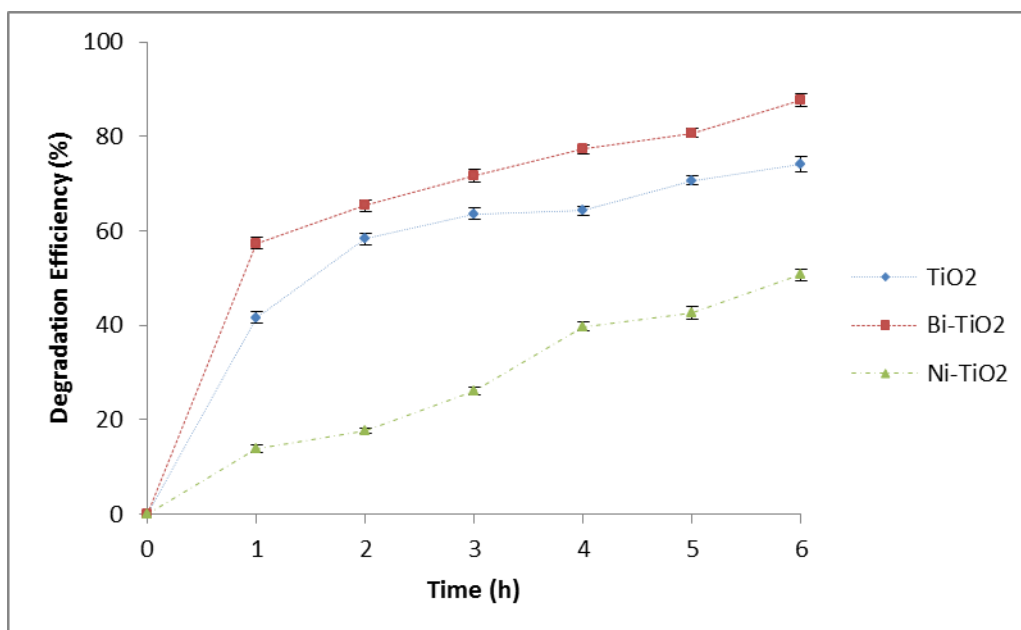


Fig. 7: Variation of Type of catalyst

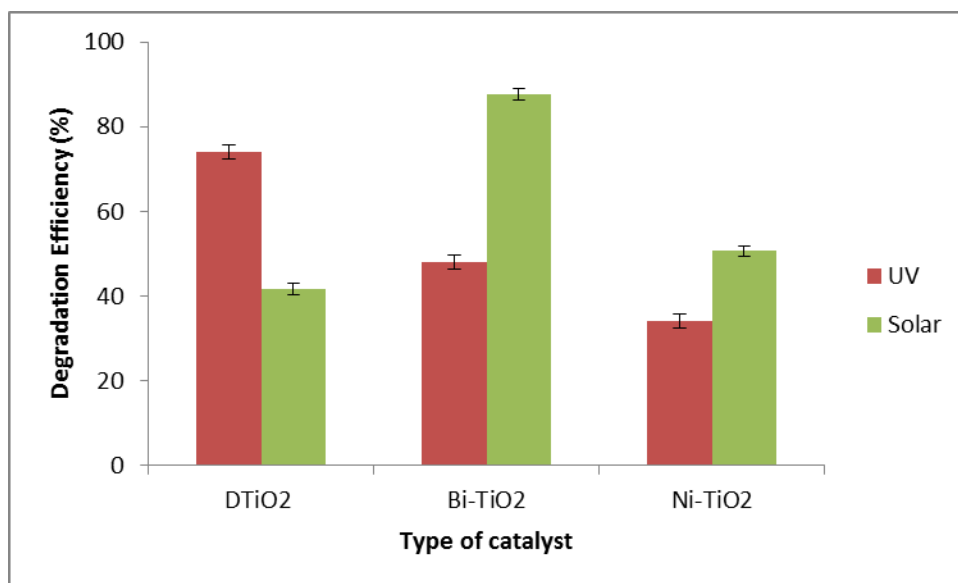


Fig 8: Variation of Light source

Tables

Table 1. EDS of various dopant concentration

Bi-TiO₂	Elements			Ni-TiO₂	Elements		
Dopant Concentration	Bi	O	Ti	Dopant Concentration	Ni	O	Ti
0.25wt%	0.21	0.02	0.02	0.25wt%	0.18	0.02	0.05
0.50wt%	0.43	0.03	0.04	0.50wt%	0.36	0.5	0.9
1.0wt%	0.88	0.20	0.10	1.0wt%	0.74	0.08	0.18

Table 2. Crystalline size and Surface area of Ni doped TiO₂

Ni (wt%)	Crystalline Size	Surface Area
0.25	13.84nm	41.71 m ² /g
0.50	10.3nm	45.7 m ² /g
1.0	16.92nm	40.8 m ² /g

Table 3. Crystalline size and Surface area of Bi doped TiO₂

Bi (wt%)	Crystalline Size	Surface Area
0.25	12.4nm	47.8 m ² /g
0.50	13.67nm	43.4 m ² /g
1.0	15.6nm	42.1 m ² /g